Spatial and Temporal Heterogeneity Explain Disease Dynamics in a Spatially Explicit Network Model

Christopher P. Brooks[1,*] Janis Antonovics,[2,†] and Timothy H. Keitt[1,‡]

1. Section of Integrative Biology, University of Texas, Austin, Texas 78712;
2. Department of Biology, University of Virginia, Charlottesville, Virginia 22904

Submitted June 15, 2007; Accepted February 27, 2008; Electronically published July 2, 2008

ABSTRACT: There is an increasing recognition that individual-level spatial and temporal heterogeneity may play an important role in metapopulation dynamics and persistence. In particular, the patterns of contact within and between aggregates (e.g., demes) at different spatial and temporal scales may reveal important mechanisms governing metapopulation dynamics. Using 7 years of data on the interaction between the anther smut fungus (*Microbotryum violaceum*) and fire pink (*Silene virginica*), we show how the application of spatially explicit and implicit network models can be used to make accurate predictions of infection dynamics in spatially structured populations. Explicit consideration of both spatial and temporal organization reveals the role of each in spreading risk for both the host and the pathogen. This work suggests that the application of spatially explicit network models can yield important insights into how heterogeneous structure can promote the persistence of species in natural landscapes.

Keywords: network epidemiology, disease ecology, biocomplexity, *Microbotryum violaceum*, *Silene virginica*.

Understanding the mechanisms by which ecological processes at one spatial and/or temporal scale affect processes at alternative scales remains one of the important challenges in ecology (Levin 1992). At any particular scale, mean field models (e.g., Anderson and May 1992; Hanski 1994, 1996) are often successful at predicting the outcome of one or several ecological processes. But there is an increasing recognition that explicit consideration of individual-level heterogeneity, both within and between scales of aggregation, may be fundamental to a mechanistic understanding of population persistence (Hanski 1996) and the spread of infectious disease (Meyers et al. 2005*b*). These individual-level heterogeneities may also suggest potential targets for the management or control of spatial spread by identifying individuals or populations within the metapopulation that are disproportionately important to overall connectivity (Hanski and Ovaskainen 2000; Brooks 2006).

One approach to the incorporation of heterogeneity is through the application of network theory. The application of these models in ecology provides a number of existing tools for quantifying individual-level heterogeneities and their effects at different spatial or temporal scales (e.g., Keitt et al. 1997; Bunn et al. 2000; Brooks 2006). Many of the existing measures and approaches to analysis have interpretations that are consistent with biological processes such as dispersal, disease transmission, and the flow of energy through trophic networks.

Construction of network models is based on discrete mathematical structures called graphs. Graphs consist of two components: vertices and edges (see recent reviews of network models in Urban and Keitt 2001; Newman 2003) that can be "decorated" with a suite of additional information. In an ecological context, vertices are typically used to represent discrete entities such as individuals or populations, while edges represent some form of interaction between them. Previous applications of network models have focused on spatially implicit models of compartmentalization in trophic structure (Dunne et al. 2002; Pascual and Dunne 2006) or the transmission of human disease based on theoretical social networks (Meyers et al. 2003, 2005*a*, 2005*b*; Newman 2005). More recently, there has been a growing interest in the characterization of the spatial structure of populations in heterogeneous landscapes using network models (Keitt et al. 1997; Bunn et al. 2000; Hanski and Ovaskainen 2000; Ferguson et al.

* Corresponding author. Present address: Department of Biological Sciences, P.O. Box GY, Mississippi State University, Mississippi State, Mississippi 39762; e-mail: cpbrooks@biology.msstate.edu.

† E-mail: ja8n@virginia.edu.

‡ E-mail: tkeitt@mail.utexas.edu.

Am. Nat. 2008. Vol. 172, pp. 149–159.
DOI: 10.1086/589451

2001; Keeling et al. 2001; Ovaskainen and Hanski 2001; Brooks 2006; Parham and Ferguson 2006; Jeger et al. 2007).

Approaches to the construction of spatial network models in population ecology can be coarsely divided into those that treat interaction as a continuous variable that decays with increasing distance (e.g., Ovaskainen and Hanski 2001) and those in which spatial constraints are represented as a binary variable (e.g., Keitt et al. 1997; Bunn et al. 2000; Brooks 2006). To date, there have been relatively few attempts to apply spatially explicit network models to empirical systems in order to identify critical mechanisms or individuals for the flow of "information" across the network. In many cases, this may be due to the difficulty in obtaining the data necessary to quantify both the scale or scales at which interactions occur and the sensitivity of model predictions to errors in network construction.

Here we explore the utility of different approaches for estimating the patterns of interaction in spatial network models. We begin by outlining the existing approaches in spatial network theory and their links with spatially realistic metapopulation theory. The patterns of anther smut (*Microbotryum violaceum*) infection within and between years in a population of fire pink (*Silene virginica*) from southwestern Virginia are then analyzed using spatially explicit network models. We illustrate the correspondence between different algorithms for estimating network structure and demonstrate the strengths of both continuous and binary edge weighting in predicting the net reproductive number (R_N) and infection prevalence in the population.

Spatial Network Theory

The underlying structure of a network model is a discrete mathematical construct called a graph. A graph $\mathcal{G}$ can be defined as a set of vertices $v_a \in \mathcal{V}$ and the set of edges $e_b \in \mathcal{E}$ that are incident to $\mathcal{V}$. Often $\mathcal{G}$ is represented as a matrix M in which rows i and columns j identify vertices, and matrix elements m_{ij} contain the strength of interaction defined by each edge. Given a set of vertices on the Euclidean plane that represent the relative spatial location of individual hosts or habitat patches, we would ideally define the edge set by quantifying the exact pattern of interaction between each pair of $v_a \in \mathcal{G}$. In natural systems such information is rarely available, and thus we must estimate $\mathcal{E}$ using our knowledge of the processes governing interaction at the individual level. The result is an estimated edge set $\hat{\mathcal{E}}$ for the graph.

There are a number of approaches that may be appropriate for generating $\hat{\mathcal{E}}$ without having explicit knowledge of each potential pairwise interaction. In many cases there exist spatial or topological constraints on interaction that can be used to estimate pairwise patterns of interaction using either binary distinctions (e.g., pairs are connected or they are not) based on their spatial and/or topological relationships or a continuous model that describes the decay of interaction with distance.

Discrete-Edge Weights

There are a number of possible ways to use relative spatial structure to estimate the flow of disease or dispersers between vertices in the model. In each case the goal is to connect the vertices in a manner that reflects the scale at which individuals interact in the system—the organism-centric scale of organization (e.g., Wiens 1989; Brooks 2003). We adopted two such approaches, one based on a distance threshold and another based on nearest-neighbor topology. The former involves identification of a threshold distance d_c that represents the mean (or maximal) distance at which interaction might be expected to occur and connect all pairs of vertices separated by no more than that distance (fig. 1*a*). This has been the most commonly applied approach to estimating $\hat{\mathcal{E}}$ for discrete binary (i.e., connections are either present or absent) spatial network models (sensu Keitt et al. 1997; Bunn et al. 2000; Brooks 2006). The latter approach is to construct $\mathcal{G}$ so that every vertex is connected only to its spatially nearest neighbors (fig. 1*b*). In this context, $\hat{\mathcal{E}}$ is constructed via a Delaunay triangulation of the points. This graph is constructed by considering only edges in which a circumscribing circle around cycles of three vertices do not include any other vertices. In both approaches, the graphs are then represented by an adjacency matrix M so that each edge is given an equivalent weight $m_{ij} = 1$, and nonexistent edges are given a weight $m_{ij} = 0$. The assumption implicit in the binary weighting of these edges is that all edges across which interaction can occur are equivalent.

Once $\mathcal{G}$ was constructed, we explored the importance of host connectivity to transmission across the network by calculating measures of vertex centrality. Three measures are of particular note here (though others may also be informative): vertex degree (k), betweenness centrality (b), and closeness centrality (c). Vertex degree is simply the number of edges that are incident to a particular vertex. When the graph is directional (a digraph), we can further distinguish between the indegree and outdegree for any vertex in $\mathcal{G}$. The distribution of k (called the degree distribution) is often used to describe the overall structure of $\mathcal{G}$. Betweenness centrality is a second measure of vertex importance and measures the number of pairwise shortest paths in $\mathcal{G}$ that pass through the focal vertex. Thus, vertices with a high value of b are those through which there is a large flow across the network. Closeness centrality is de-

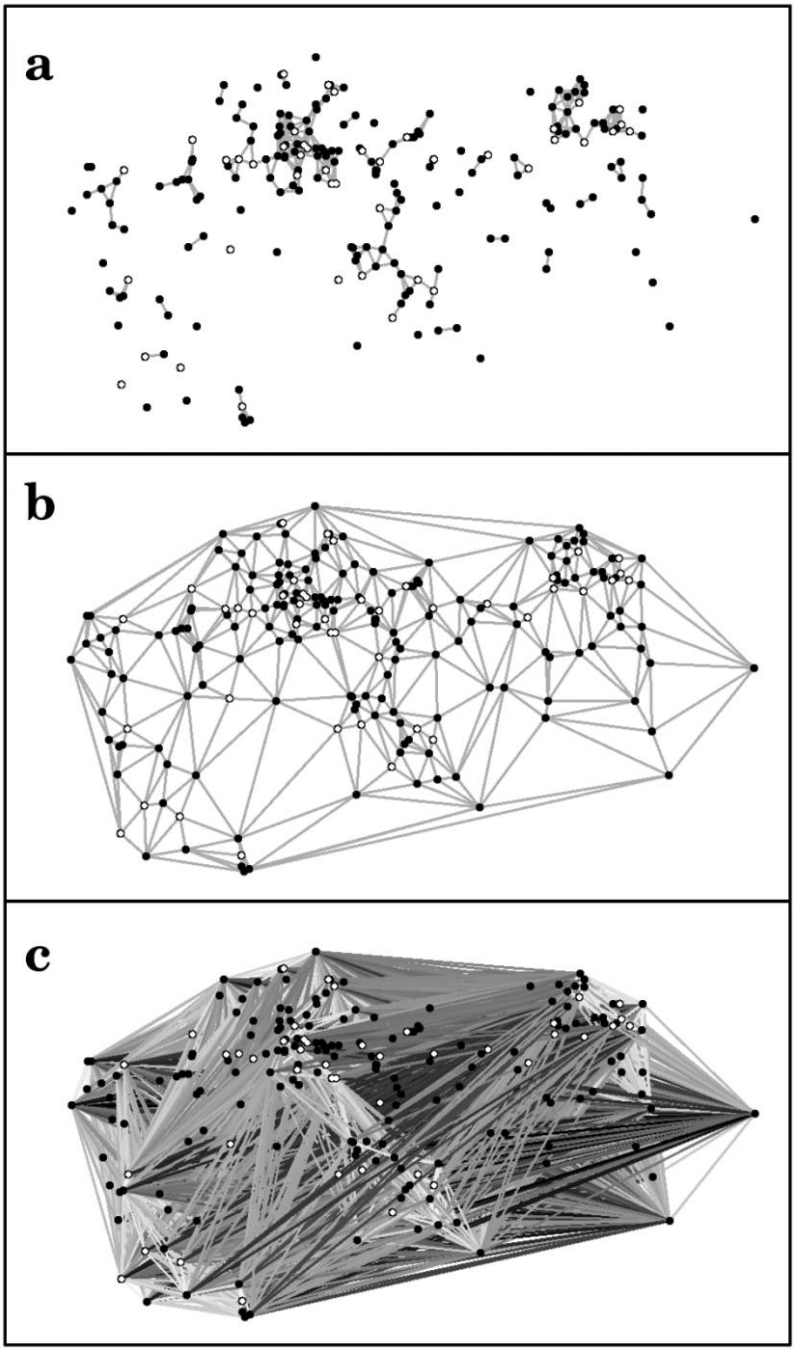

Figure 1: Examples of networks based on (*a*) a distance threshold of 0.92*m*, (*b*) nearest-neighbor topology, or (*c*) distance-weighted edges for all possible pairings (metapopulation model) for the spatial arrangement of *Silene virginica* at the Morrisette Winery in southwestern Virginia in 1990. Open circles represent individuals that were infected in a particular year, filled circles represent healthy individuals, and lines represent edges that connect potentially interacting flowers in the population. Strength of interaction (*c*) is denoted by the degree of shading, with lighter colors indicating stronger interactions.

fined as the mean number of edges (calculated through shortest paths) that have to be traversed to move between the focal vertex and every other vertex in the graph. This means that the value of closeness is inverted relative to what one might logically interpret from the name; high values indicate a low centrality for a particular vertex. Here we construct $\hat{\mathcal{E}}$ by considering topological or spatial constraints on the transmission of *Microbotryum violaceum* between hosts. If transmission occurs at a particular spatial scale, then the patterns of centrality in the network constructed using that critical distance should provide an accurate prediction of transmission (e.g., Brooks 2006).

Continuous-Edge Weights

When the strength of interaction between any pair of vertices is critical to our understanding of flow across the network, we can weight edges with a continuous function that describes the decay of interaction with distance (fig. 1*c*). Although we can construct graphs in which we consider both the topology of actual interactions in the system and the decay function (Urban and Keitt 2001; Keitt 2003), most continuous-network models ignore the topological heterogeneity in the network and simply model the interaction for all $v \in \mathcal{G}$. This is, very generally, the approach used in constructing spatially realistic metapopulation models (sensu Hanski and Ovaskainen 2000; Ovaskainen and Hanski 2001). The decay of interaction strength with distance can be described by any function, but for metapopulation models it is generally described as

$$m_{ij} = A_i A_j \exp(-\alpha d_{ij}), \tag{1}$$

where A_x is the area of patch x, d_{ij} is the distance between the vertices defined by column i and row j in an adjacency matrix M, and α is the inverse of the mean dispersal distance for the species whose movement is being modeled (Hanski 1994). The dominant eigenvalue of this matrix of edge weights λ_M then provides an estimate of the available habitat for the metapopulation or the metapopulation capacity (Hanski and Ovaskainen 2000; Ovaskainen and Hanski 2001). Because λ_M is a measure of the available habitat, we can predict the proportion of available habitat occupied at equilibrium as

$$p^* = 1 - \phi\lambda^{-1}, \tag{2}$$

where ϕ is the ratio of extinction to colonization rates (Hanski and Ovaskainen 2000).

The Empirical Model System

In order to assess the power and robustness of spatial network approaches in predicting population dynamics, we constructed a series of empirically derived networks to describe the transmission dynamics of the anther smut fungus (*Microbotryum violaceum*) in a population of fire pink (*Silene virginica*) between 1989 and 1995. These data describe the location and disease status of each *S. virginica* individual within a 30 × 35-m study plot in southwestern Virginia (Morrisette Winery site) during the flowering season (Antonovics et al. 1996). Vertex sets were constructed using both the relative spatial location and infection status of each scored individual. Vegetative plants were excluded from the analysis because they are unlikely to affect the behavior of pollinators that transmit the disease from plant to plant (Antonovics et al. 1996). Given the location and disease status of all individuals in the plot, we estimated $\hat{\mathcal{E}}$ using all of the approaches described in the previous section in an effort to evaluate how well each predicts the spatial and temporal patterns in prevalence and transmission of the fungal pathogen.

The Study System

Silene virginica is a short-lived perennial plant that is among the most conspicuous wildflowers from May to June in the central and southeastern United States. Infection results in the development of anthers that contain fungal spores instead of pollen grains, in a manner that is similar to its invasive congener *Silene latifolia* (Baker 1947). Unlike infection in *S. latifolia*, however, dark anthers and the deep red of the flowers in *S. virginica* make infection far less conspicuous (Antonovics et al. 2003). Pollination of fire pink is mediated largely by ruby-throated hummingbirds, with some contribution from solitary bees (Fenster and Dudash 2001). As in other members of the genus, infection is assumed to spread between individuals via two primary routes. Visits by pollinators to an infected flower result in the acquisition of teliospores that are transferred to healthy flowers as the pollinator moves through the population (Baker 1947; Alexander 1990; Antonovics and Alexander 1992; Roche et al. 1996; Altizer et al. 1998). Seedlings and vegetative individuals may also become infected through aerial transmission of spores from nearby infected flowers (Alexander 1990). Because pollinators are likely to deposit most of their spores on the first few visits after acquiring teliospores, we expect that infection should be highly localized (sensu Giraud 2004). There are also strong temporal constraints: because transmission is restricted to the flowering phenology, there is a distinct 3–4-week transmission period each year. We calculated the growth rate of infection as the net repro-

ductive number R_N, defined as the number of new infections per infection in each year,

$$R_N(t) = \frac{I(t)}{I(t-1)}. \quad (3)$$

Because we were able to identify individuals between years, it was also possible to determine the number of newly established individuals (where establishment indicates survival to first flowering), the survivorship of diseased and healthy individuals, and which hosts were newly infected during each flowering season.

Graph Construction Algorithms

To measure the influence of spatial structure on the spread of the fungal pathogen in the system, we constructed a series of graphs using the relative location of individual plants as vertices. Here vertices possess (x, y) coordinates in the plane as well as a disease status (susceptible S or infectious I). Because data describing the exact paths of movement and spore deposition for pollinating insects are not available, we adopted three approaches for estimating $\hat{\mathcal{E}}$, two discrete and one continuous. The continuous-edge weight graph was based on existing metapopulation models (e.g., Hanski and Ovaskainen 2000; Ovaskainen and Hanski 2001) in which interaction between hosts is a decaying function of distance. Because we lack information on the size of individual flowers or plants, we assume $A_i = A_j = 1$ and calculate the entries of M as in equation (1). It was also necessary to estimate the critical distance beyond which transmission is unlikely to occur. As with *S. latifolia* insect pollinators, we expect that most teliospores will be deposited on the first few flowers visited by a pollinator (Altizer et al. 1998). So, despite the differences in the community of pollinators between *S. virginica* and *S. latifolia*, we expect that infection will be similarly distributed. Thus we construct edges based on the assumption that transmission occurs within a critical distance of $d_c = 0.92m$ (fig. 1*a*). This is based on the scale of spatial autocorrelation in the clustering of paired infections (sensu Real and MacElhaney 1996; Brooks 2006), a measure that may be especially important in tracking epidemics on spatially explicit networks (Bauch and Galvani 2003). Assuming an exponential decay of interaction (sensu eq. [1]), this implies a rate parameter for equation (1) and the continuously weighted graphs of $\alpha = 3.25$.

Two graphs were also constructed where host-host interaction was considered as a binary variable. In one, we considered all of the topological nearest neighbors of any living flower to be interconnected irrespective of interhost distances (fig. 1*b*). This was constructed as the Delaunay triangulation of the vertices that results in a connected graph (all vertices are part of a single connected component) of the plant locations on a two-dimensional plane. The Delaunay triangulation for a set of points requires that for every cycle with only three edges, there is a circumcircle (circle that includes each vertex along its edge) that has no other vertices inside it. The result is a graph that includes connections between topologically nearest neighbors. A third graph was based on the assumption that all vertices within some critical threshold distance of one another are interconnected (e.g., Keitt et al. 1997; Brooks 2006; fig. 1*c*). As with the critical distance used in calculating α, we use $d_c = 0.92m$ as the threshold for constructing this final class of graphs. These approaches were chosen to represent three of the potential algorithms among many that are possible (Urban and Keitt 2001; Keitt 2003).

We also constructed a spatiotemporal graph in an effort to evaluate the importance of year-to-year variation in spatial structure on the transmission of *Microbotryum violaceum*. This spatiotemporal network is based on the distance-threshold graphs with $d_c = 0.92m$. For each pair of adjacent years, we identified individuals that were alive in year t and in year $t + 1$. Because we did not have information on the disease status of vegetative individuals, we restricted our analysis to those individuals that were flowering in both year t and year $t + 1$. We then accounted for the year-to-year survival of individuals and considered all spatial edges for each individual in each of the years that it was alive (and flowering). This generates a structure in which the network accounts for the spatial arrangement of individuals both within and between years.

Network Analysis

For each of the discrete spatial graphs, we calculated three measures of vertex centrality: vertex degree, betweenness centrality, and closeness centrality for all plants and separately for infected and healthy plants. Each of these measures captures different elements about the biology of the system that may be important to the transmission of *M. violaceum*. The degree distribution (distribution of the number of edges incident to each vertex or the neighborhood size of each vertex) was calculated for nearest-neighbor graphs as a measure of the overall structure of the spatial network. This measure was calculated across the network as a whole (diseased and healthy individuals) and separated by disease class for any particular year (e.g., the number of healthy and infected hosts connected to each diseased host, the number of diseased or healthy hosts connected to each susceptible host, etc.). This allows for the calculation of the number of healthy neighbors for each infected host—a measure that is likely to be important if infection occurs via stepping-stone-type movement.

For each of the other measures of centrality, we calculated a mean value for each disease class. This value is the mean centrality of vertices of class *c* relative to all other vertices in the network. Betweenness centrality measures the number of pairwise shortest paths between vertices in the graph that pass through any particular vertex. If infection "flows" across the network along the most efficient paths in space (something we might expect of pollinator behavior), then we might expect betweenness centrality to predict the pattern of disease spread. Closeness centrality should reveal the degree to which there is localization of transmission in space. It provides a measure that is somewhat similar to vertex degree, but it can reveal the effects of clustering within neighborhoods of more than one step.

The ability of these models to predict spatiotemporal patterns of infection and transmission in the system was evaluated across years using general linear modeling in the R statistical package (R Development Core Team 2006). Analysis of the continuously weighted graphs was restricted to an exploration of spatially realistic metapopulation theory, using standard exponential decay of interaction with increasing distance (Hanski and Ovaskainen 2000; Ovaskainen and Hanski 2001) and an assessment of the potential of metapopulation capacity (λ_M) to predict the prevalence and dynamics of infection in the system.

Results

Over the study period the number of plants in the study plot ranged from 125 in 1989 to 257 in 1991. The patterns of fluctuation and the number of new infections suggest a generally low transmission rate (Antonovics et al. 1996) punctuated by two outbreaks ($R_0 > 1$) of the fungal pathogen, in 1990 and 1993. The second outbreak followed a severe decline in the host population (>30% mortality in the population between 1991 and 1992) and a subsequently high recruitment of susceptible flowers at the start of the transmission season in 1993. Initially we tested a simple discrete-time susceptible-infected-type model that overpredicted the amount of infection in the system ($I_{t+1} = \beta S_t I_t - \mu I_t$; $P > .7$).

Discrete-Network Models

Results from the two discrete-network models were qualitatively similar, though those based on the threshold distance were slightly better predictors of R_N than the nearest-neighbor graphs. Examples of the distance-threshold, nearest-neighbor, and metapopulation graphs are shown in figure 1. We focus on the results from distance-threshold graphs here and highlight results for the nearest-neighbor graphs that are of note.

The number of neighbors for each of the plants in the system (both healthy and infected) was highly variable both within and across years (fig. 2). When there were infected hosts that were highly connected ($k > 10$), $R_N > 1$, the threshold for epidemic growth. However, the number of susceptible hosts that were directly connected to infected hosts was not predictive of R_N. Topology was a better predictor of infection rate in the distance-threshold graphs. Betweenness centrality (the number of shortest paths that include a particular host [vertex]) of infected hosts was also highly predictive of R_N and the prevalence of infection. The mean betweenness centrality of infected vertices $\bar{b}_I$ in year t explained 73.3% of the variation observed in R_N in the following year (fig. 3*a*). Mean closeness centrality of infected vertices $\bar{c}_I$ in the threshold graphs during year t were also good predictors of R_N. The mean number of "steps" between all hosts and at least one infected host explained 78.4% of the variation in R_N in year t (fig. 3*b*). Unlike $\bar{b}_I$, closeness was not able to forecast the dynamics of infection in the system a season in advance.

It is important to note here that the distance-threshold networks are highly disconnected at $d_c = 0.92m$ in each year of the study period. Typically, network metrics are used on connected structures (a network in which all vertices are a part of a single connected component). If the disconnected nature of these threshold graphs were an accurate reflection of the spatial spread of infection, we might expect to see a correspondence between the clustering of infection in the spatial network and the topology of the more connected structure (e.g., the centrality of infection in the nearest-neighbor graph). Using networks constructed for the $0.92m$ threshold, we found that the mean betweenness centrality, $\bar{b}_I$, for the nearest-neighbor graphs was highly predictive of the number of edges connecting pairs of infected hosts in the distance-based graph ($r^2 = 0.98$; $P < .0001$).

We can measure the degree of connectedness in the distance-threshold network by plotting the mean size of clusters that are connected at a given critical distance, d_c. This edge-thinning technique provides a visual representation of the overall spatial connectivity in the network. We also explored the degree to which the survival of and flowering by both infected and healthy individuals across multiple years affected the spatiotemporal patterns of connectivity in the system. Comparison of the changes in connectivity for the spatiotemporal network versus the spatial networks constructed for each year (fig. 4) shows that temporal changes in spatial structure have a large effect on connectivity.

Continuous-Network Model

The continuous-network model provided an excellent prediction of infection prevalence in each year. The propor-

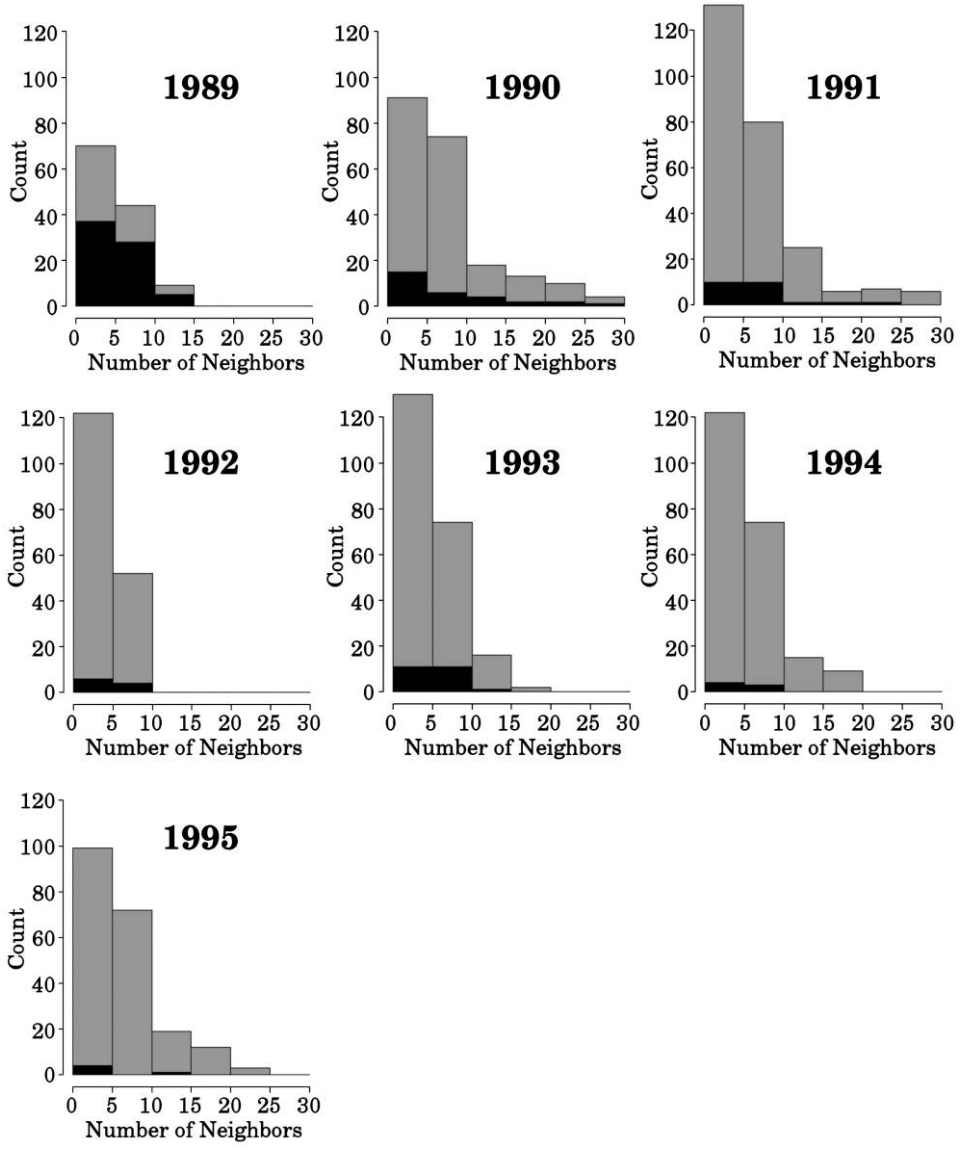

Figure 2: Distribution of neighbors for each vertex based on the distance-threshold graphs with critical distance $d_c = 0.92m$. Black sections of the histogram indicate infected individuals; gray sections indicate healthy individuals.

tion of hosts infected (i.e., proportion of patches occupied) at equilibrium, as predicted by equation 2, explained 96.2% of the variance in observed infection prevalence. The least squares estimate of the ratio of extinction : colonization rate $\phi = 3.84$ from this model suggests a decline in the pathogen population over time.

This metapopulation network model also predicts the net reproductive number for the pathogen, though not as well as the models with discrete-edge weights. Capacity (λ_M) is a measure of host availability for existing infections (Hanski and Ovaskainen 2000; Ovaskainen and Hanski 2001). As a result, the ratio of capacities reflects the change in the availability of susceptible hosts between years. The ratio of metapopulation capacities between years $\lambda_M(t)/\lambda_M(t-1)$ explained >60% of the variation in R_N ($P = .05$).

Discussion

Together the predictive patterns in both the continuous and discrete binary graphs suggest that the interactions between host and pathogen (as mediated by the pollinator)

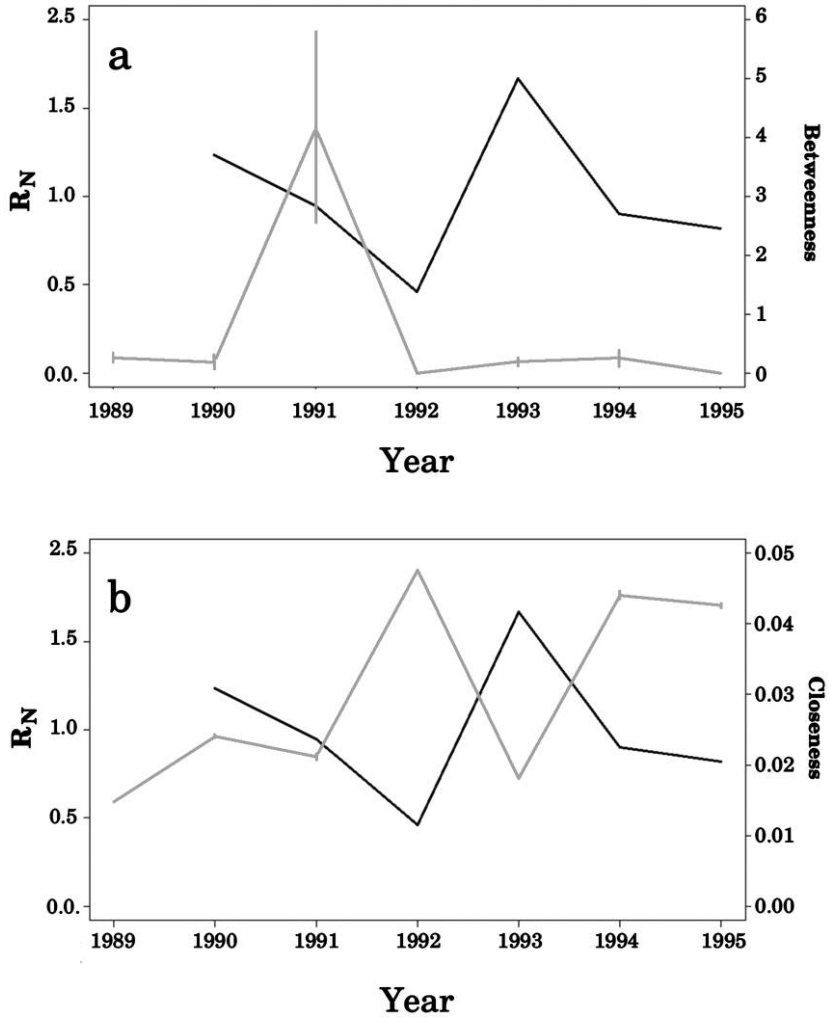

Figure 3: Temporal trends in mean (*a*) betweenness and (*b*) closeness centrality of infected vertices (*gray line*) and R_N (*black line*) for each year. Vertical lines are 1 SE from the mean.

occur via a consistent spatial pattern across years. Most of the variation in infection between years is a direct result of birth, death, and infection altering the spatial distribution of susceptible flowering hosts. The effect of removing individuals due to immunity, infection, or death from a heterogeneous contact network may ultimately alter the pattern and rate of transmission during the course of an outbreak (Ferrari et al. 2006). Here there is little recovery, and there is no apparent mortality cost of infection (Antonovics et al. 1996). Infection alters only the location of susceptible individuals and the spatial pattern of future births and deaths through the parasitic castration of infected flowers. The remaining spatial pattern in susceptible hosts is a result of natural birth-death processes operating in the system. As a result, infection becomes highly aggregated relative to the overall spatial distribution of hosts (Antonovics et al. 1996). The scale at which hosts are aggregated in a patch relative to the spatial spread of *Microbotryum violaceum* implies that only hosts that are in locally connected clusters that contain infected plants are likely to be infected. Thus, in any particular year, the risk of infection is isolated in a subset of the clusters in the population, thereby preventing widespread transmission in any one year (e.g., den Boer 1968). The result is that some susceptible individuals will always have a much lower probability of infection than others (e.g., the contact heterogeneity) within a season.

The patterns of *M. violaceum* transmission in this population of *Silene virginica* are best explained through explicit consideration of this contact heterogeneity in the

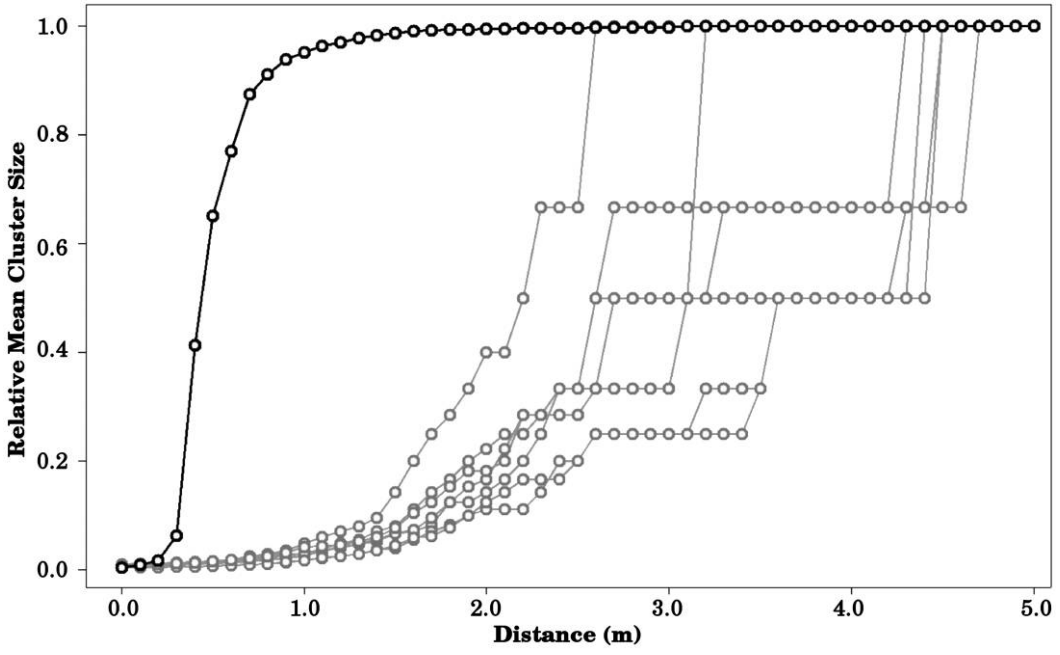

Figure 4: Edge-thinning plot showing the change in the mean size of connected clusters as a function of threshold distance (d_c) for each year independently (*gray*) and for the spatiotemporal network model that also considers survival between years (*black*).

system. Network models based on binary weighting of edges were especially good at explaining variation in R_N up to one season in advance. The metapopulation network model was also capable of explaining variation in R_N, but it was especially good at predicting infection prevalence in the flowering population. The accuracy of this equilibrium prediction of prevalence (eq. [2]) from metapopulation theory suggests that infection is constrained by the spatial topology of hosts in the population, probably due to behavioral tendencies in the pollinators. Thus, the paths along which infection spreads are likely to be traversed many times throughout the transmission season. This results in numerous opportunities throughout the season for pathogen transmission to highly connected individuals.

The measures of vertex centrality suggest a progression of events by which the risk of hosts is spread in the network. The initial increase in the betweenness centrality of infected hosts that signals a coming epidemic reflects an initial stage in which infection is distributed in clusters that lie along many of the shortest paths between hosts. In this case, the importance of shortest paths is not surprising given that hummingbirds are generally likely to follow the shortest paths between neighboring flowers when feeding (e.g., Wolf and Hainsworth 1990). Once the pollinators acquire teliospores from an infected host and spread them along these paths, infection becomes more widespread in the network, thereby colonizing clusters of hosts that might have previously escaped infection. The result is that the parasite then lies only a few steps from all of the other individuals in the population at the start of the next transmission season.

It seems clear that the risk of infection varies across space as a function of who your neighbors are and what their disease status is in any season. Temporal variation in host spatial structure slows the spatial spread of the pathogen in any single season, reducing the pathogen's risk of extinction due to overexploitation of the local pool of susceptible hosts in a single season while allowing for efficient transmission within localized clumps in susceptible hosts. We observed infection spreading rapidly through small, isolated aggregations of susceptible hosts during individual seasons, with the spatial extent of the spread being mediated by the degree of connectivity across the network in any particular year. Survival of individuals, and their infections between years, imparts a "memory" in the system that interacts with the new structure resulting from births and deaths between the end of one transmission season and the beginning of the next. It is the temporal connection mediated by a few individuals that allows the parasite to infect hosts across previously separate aggregates and to "scale-up" the infection to explain the transmission between these clusters.

Our study illustrates the ability of spatial network models to accurately predict transmission rate when interaction

among hosts is highly heterogeneous. We expect that the construction of species-specific network models based on movement ability will be particularly useful in designing habitat reserves as well as in controlling the spread of invasive species such as the cactus moth (*Cactoblastis cactorum*) in North America. This analysis is based on a model system, and the degree to which the results in this system might apply to other natural systems remains an open question. These spatially explicit network models may be useful in conservation ecology as well as in forestry, but their application will require careful analysis of the possible methods of edge construction and of the assumptions about the ecology of the system represented by each approach.

Acknowledgments

We would like to thank the many people who helped with the fieldwork, including H. Alexander, A. Davelos, M. Heuhsen, M. Hood, A. Jarosz, D. Stratton, S. Taliaferro, D. Taylor, and P. Thrall. The study was partly supported by National Science Foundation grant DEB-9119626, and we are grateful to the National Park Service for permission to carry out studies on the Blue Ridge Parkway. The Keitt lab acknowledges the support of the David and Lucile Packard Foundation and the Texas Space Grant Consortium funded by the National Aeronautics and Space Administration. Thanks also to the Mike Boots lab and two anonymous reviewers for comments that greatly improved the quality of this manuscript.

Literature Cited

Alexander, H. M. 1990. Epidemiology of anther-smut infection of *Silene alba* caused by *Ustilago violacea*: patterns of spore deposition and disease incidence. Journal of Ecology 78:166–179.

Altizer, S. M., P. H. Thrall, and J. Antonovics. 1998. Vector behavior and the transmission of anther-smut infection in *Silene alba*. American Midland Naturalist 139:147–163.

Anderson, R. M., and R. M. May. 1992. Infectious diseases of humans: dynamics and control. Oxford University Press, Oxford.

Antonovics, J., and H. M. Alexander. 1992. Epidemiology of anther-smut infection of *Silene alba* (= *S. latifolia*) caused by *Ustilago violacea*: patterns of spore deposition in experimental populations. Proceedings of the Royal Society B: Biological Sciences 250:157–163.

Antonovics, J., D. Stratton, P. H. Thrall, and A. M. Jarosz. 1996. An anther-smut disease (*Ustilago violacea*) of fire-pink (*Silene virginica*): its biology and relationship to the anther-smut disease of white campion (*Silene alba*). American Midland Naturalist 135: 130–143.

Antonovics, J., M. E. Hood, P. H. Thrall, J. Y. Abrams, and G. M. Duthie. 2003. Herbarium studies on the distribution of anther-smut fungus (*Microbotryum violaceum*) and *Silene* species (Caryophyllaceae) in the eastern United States. American Journal of Botany 91:1522–1531.

Baker, H. G. 1947. Infection of species of *Melandrium* by *Ustilago violacea* (pers.) Fuckel and the transmission of the resultant disease. Annals of Botany 11:333–348.

Bauch, C. T., and A. P. Galvani. 2003. Using network models to approximate spatial point processes. Mathematical Biosciences 184:101–114.

Brooks, C. P. 2003. A scalar analysis of landscape connectivity. Oikos 102:433–439.

———. 2006. Quantifying population substructure: extending the graph-theoretic approach. Ecology 87:864–872.

Bunn, A. G., D. L. Urban, and T. H. Keitt. 2000. Landscape connectivity: a conservation application of graph theory. Journal of Environmental Management 59:265–278.

den Boer, P. J. 1968. Spreading of risk and stabilization of animal numbers. Acta Biotheoretica 18:165–194.

Dunne, J. A., R. J. Williams, and N. D. Martinez. 2002. Food-web structure and network theory: the role of connectance and size. Proceedings of the National Academy of Sciences of the USA 99: 12917–12922.

Fenster, C. B., and M. R. Dudash. 2001. Spatiotemporal variation in the role of hummingbirds as pollinators of *Silene virginica*. Ecology 82:844–851.

Ferguson, N., C. Donnelly, and R. Anderson. 2001. The foot and mouth epidemic in Great Britain: pattern of spread and impact of interventions. Science 292:1155–1160.

Ferrari, M. J., S. Bansal, L. A. Meyers, and O. N. Bjørnstad. 2006. Network frailty and the geometry of herd immunity. Proceedings of the Royal Society B: Biological Sciences 273:2743–2748.

Giraud, T. 2004. Patterns of within population dispersal and mating of the fungus *Microbotryum violaceum* parasitising the plant *Silene latifolia*. Heredity 93:559–565.

Hanski, I. 1994. A practical model of metapopulation dynamics. Journal of Animal Ecology 63:151–162.

———. 1996. Metapopulation dynamics: from concepts and observations to predictive models. Pages 69–91 *in* I. Hanski and M. E. Gilpin, eds. Metapopulation biology: ecology, genetics and evolution. Academic Press, New York.

Hanski, I., and O. Ovaskainen. 2000. The metapopulation capacity of a fragmented landscape. Nature 404:755–758.

Jeger, M. J., M. Pautasso, O. Holdenrieder, and M. W. Shaw. 2007. Modeling disease spread and control in networks: implications for plant sciences. New Phytologist 174:279–297.

Keeling, M. J., M. E. J. Woolhouse, D. J. Shaw, L. Matthews, M. Chase-Topping, D. T. Haydon, S. J. Cornell, J. Kappey, J. Wilesmith, and B. T. Grenfell. 2001. Dynamics of the 2001 UK foot and mouth epidemic: stochastic dispersal in a heterogeneous landscape. Science 294:813–817.

Keitt, T. H. 2003. Network theory: an evolving approach to landscape conservation. Pages 125–134 *in* V. H. Dale, ed. Ecological modeling for resource management. Springer, New York.

Keitt, T. H., D. L. Urban, and B. T. Milne. 1997. Detecting critical scales in fragmented landscapes. Conservation Ecology vol. 1, article 4.

Levin, S. A. 1992. The problem of pattern and scale in ecology. Ecology 73:1943–1967.

Meyers, L. A., M. E. J. Newman, M. Martin, and D. Schrag. 2003. Applying network theory to epidemics: control measures for *Mycoplasma pneumoniae* outbreaks. Emerging Infectious Diseases 9: 204–210.

Meyers, L. A., B. Pourbohloul, M. E. J. Newman, D. M. Skowronski,

and R. C. Brunham. 2005*a*. Network theory and SARS: predicting outbreak diversity. Journal of Theoretical Biology 232:71–81.

Meyers, L. A., M. E. J. Newman, and B. Pourbohloul. 2005*b*. Predicting epidemics on directed contact networks. Journal of Theoretical Biology 240:400–418.

Newman, M. E. J. 2003. The structure and function of complex networks. SIAM Review 45:167–256.

———. 2005. Threshold effects for two pathogens spreading on a network. Physical Review Letters 95:108701.

Ovaskainen, O., and I. Hanski. 2001. Spatially structured metapopulation models: global and local assessment of metapopulation capacity. Theoretical Population Biology 60:281–302.

Parham, P. E., and N. M. Ferguson. 2005. Space and contact networks: capturing the locality of disease transmission. Journal of the Royal Society Interface 3:483–493.

Pascual, M., and J. A. Dunne. 2006. Ecological networks: linking structure to dynamics in food webs. Oxford University Press, New York.

R Development Core Team. 2006. R: a language and environment for statistical computing. R Foundation for Statistical Computing, Vienna, ISBN 3-900051-07-0.

Real, L. A., and P. MacElhaney. 1996. Spatial pattern and process in plant-pathogen interactions. Ecology 77:1011–1025.

Roche, B. M., H. M. Alexander, and A. D. Maltby. 1996. Dispersal and disease gradients of anther smut infection of *Silene alba* at different life stages. Ecology 76:1863–1871.

Urban, D., and T. H. Keitt. 2001. Landscape connectivity: a graph-theoretic perspective. Ecology 82:1205–1218.

Wiens, J. A. 1989. Spatial scaling in ecology. Functional Ecology 3: 385–397.

Wolf, L. L., and F. R. Hainsworth. 1990. Non-random foraging by hummingbirds: patterns of movement between *Ipomopsis aggregata* inflorescences. Functional Ecology 4:149–157.

Associate Editor: Matthew J. Keeling
Editor: Donald L. DeAngelis

Healthy and infected individuals of fire pink (*Silene virginica*). Infection is spread between flowers by pollinators. (Photographs by J. Antonovics.)